Title

Insights into Photosynthetic Energy Transfer Gained from Free-Energy Structure: Coherent Transport, Incoherent Hopping, and Vibrational Assistance Revisited

Journal

The Journal of Physical Chemistry B, 125(13)

ISSN

1520-6106

Authors

Ishizaki, Akihito
Fleming, Graham R

Publication Date

2021-04-08

DOI

10.1021/acs.jpcb.0c09847

Peer reviewed

THE JOURNAL OF PHYSICAL CHEMISTRY B
A JOURNAL OF THE AMERICAN CHEMICAL SOCIETY

pubs.acs.org/JPCB

Article

Insights into Photosynthetic Energy Transfer Gained from Free-Energy Structure: Coherent Transport, Incoherent Hopping, and Vibrational Assistance Revisited

Published as part of The Journal of Physical Chemistry virtual special issue "Yoshitaka Tanimura Festschrift".

Akihito Ishizaki* and Graham R. Fleming*

Cite This: *J. Phys. Chem. B* 2021, 125, 3286−3295

Read Online

ACCESS | Metrics & More | Article Recommendations

ABSTRACT: Giant strides in ultrashort laser pulse technology have enabled real-time observation of dynamical processes in complex molecular systems. Specifically, the discovery of oscillatory transients in the two-dimensional electronic spectra of photosynthetic systems stimulated a number of theoretical investigations exploring the possible physical mechanisms of the remarkable quantum efficiency of light harvesting processes. In this work, we revisit the elementary aspects of environment-induced fluctuations in the involved electronic energies and present a simple way to understand energy flow with the intuitive picture of relaxation in a funnel-type free-energy landscape. The presented free-energy description of energy transfer reveals that typical photosynthetic systems operate in an almost barrierless regime. The approach also provides insights into the distinction between coherent and incoherent energy transfer and the criteria by which the necessity of the vibrational assistance is considered.

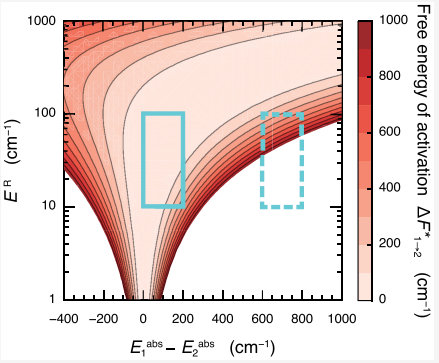

INTRODUCTION

The development of new techniques of ultrafast spectroscopy has enabled real-time observation of dynamical processes in complex chemical, biological, and material systems. In the past decade, third-order nonlinear spectroscopic techniques such as two-dimensional (2D) Fourier-transformed photon echo spectroscopy were applied to explore photosynthetic light harvesting processes,[1,2] and the existence of long-lasting oscillatory transients in 2D spectra was revealed.[3−5] Although earlier work found coherent beats with the use of pump−probe techniques,[6] the newer experiments stimulated a rapid increase in the number of experimental and theoretical investigations to explore possible roles that quantum effects may play in the remarkable quantum efficiency of light harvesting processes in natural and artificial systems.[7−54]

Initially, the beats were interpreted as signatures of quantum superpositions between delocalized energy eigenstates (electronic excitons) of excited pigments, and it was argued that the unexpectedly slow dephasing could enhance the efficiency of electronic energy transfer (EET). However, it has become clear that the experimentally observed oscillations have dephasing time that persists for much longer than the theoretically predicted electronic coherence lifetime, particularly at cryogenic temperatures.[11,14] Hence, the possibility of vibrational contributions was addressed.[55−61] A plausible explanation for the moderately long-lived spectral beats was that a quantum mixture between the electronic states and the Franck−Condon active vibrational states serves to create vibronic exciton states and produce oscillations that exhibit picosecond dephasing times,[60] while very long-lived beats likely arise from ground-state vibrational wave packets.[61] Furthermore, oscillatory transients in the 2D electronic spectra of the photosystem II reaction center were observed,[62,63] suggesting that the electronic−vibrational resonance might represent an important design principle for enabling charge separation with high quantum efficiency in oxygenic photosynthesis. However, it was questionable whether such electronic−vibrational mixtures could be robust and could play a role under the influence of protein-induced fluctuations at physiological temperatures. By using quantum dynamics calculations, it was demonstrated that such electronic−vibrational quantum mixtures do not necessarily play a significant role in the energy transfer and charge separation dynamics, despite contributing to the enhancement of long-lived beating in 2D electronic spectra.[64−67] Given the variety of pigment types and range of energy gaps in natural light

Received: November 1, 2020
Revised: February 22, 2021
Published: March 16, 2021

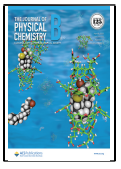

https://doi.org/10.1021/acs.jpcb.0c09847
J. Phys. Chem. B 2021, 125, 3286−3295

harvesting systems, it is not possible to make completely general statements regarding the roles of intramolecular vibrations upon photosynthetic energy/charge transfer. However, the results of refs 64−67 suggest the need for further examination on the relevance of information provided by the oscillatory behaviors in the 2D data on the studied systems and dynamics.

As stated above, quantum dynamics calculations have helped us elucidate the nature of the experimentally observed signals. However, the theories employed have reached a high degree of sophistication and have become correspondingly complex,[68−81] making it difficult to draw broadly applicable conclusions about biologically significant questions regarding the physical origin of the remarkable speed and efficiency of photosynthetic light harvesting. For example, (1) what is the key distinction between coherent and incoherent energy transfer? Does the absence of observable beats necessarily imply that the energy transfer is incoherent hopping? (2) What do the answers to these questions imply regarding the physical origin of the remarkable speed and efficiency of photosynthetic light harvesting? (3) Theoretical approaches generally assume ultrafast initial excitation, meaning that the ensemble begins its evolution in phase. What is the difference, if any, between ultrafast laser excitation and excitation by sunlight?

In this paper, we try to describe a way of understanding and visualizing the energy flow in pigment−protein complexes (PPCs) that connects the somewhat complex quantum dynamical theories to the intuitive picture of relaxation in a funnel-type free-energy landscape with respect to environment-induced fluctuations. It should be noted that EET dynamics are not directly computed with the free-energy surfaces. However, the free-energy profile can provide us with insights into the environment-induced fluctuations governing the energy transfer processes. One may recall that free-energy profiles are still useful for understanding condensed phase electron transfer reactions although microscopic formulations of environmental dynamics modify the Marcus rate formula that is characterized with the free-energy profiles.[82−86] The free-energy description of energy transfer reveals that photosynthetic systems operate in a barrierless regime when absorption energy differences among pigments are $\lesssim$200 cm^{-1}. This situation is found, for example, in the Fenna−Matthews−Olson (FMO) complex.[1,2,87] This makes the initial condition rather unimportant, suggesting that the method of excitation will not play a significant role in determining the microscopic dynamics. The free energy also provides insight into the importance of the vibrational contributions and the distinction between coherent and incoherent energy transfer, showing that the absence of observable beats in the spectroscopy does not necessarily imply that the energy transfer occurs by incoherent hopping.

THEORETICAL BACKGROUND

Hamiltonian of a Pigment−Protein Complex. To describe EET, we restrict the electronic spectra of the mth pigment in a PPC to the ground state, $|\varphi_{mg}\rangle$, and the first excited state, $|\varphi_{me}\rangle$, although higher excited states may result in nonlinear spectroscopic signals. Thus, the Hamiltonian of a PPC comprising N pigments is expressed as

$$\hat{H}_{\mathrm{PPC}} = \sum_{m=1}^{N} \sum_{a=\mathrm{g,e}} \hat{H}_{ma}(x_m)|\varphi_{ma}\rangle\langle\varphi_{ma}| + \sum_{m=1}^{N}\sum_{n=1}^{N} J_{mn}|\varphi_{me}\rangle|\varphi_{ng}\rangle\langle\varphi_{mg}|\langle\varphi_{ne}|$$

Here, $\hat{H}_{ma}(x_m)$ represents the diabatic Hamiltonian for the environmental and intramolecular vibrational degrees of freedom (DoFs), x_m, when the system is in the $|\varphi_{ma}\rangle$ state for a = g and a = e. The electronic coupling between the pigments, J_{mn}, may also be modulated by the environmental and nuclear DoFs. In the following, however, it is assumed that the nuclear dependence of J_{mn} is vanishingly small and the Condon-like approximation is employed as usual. The Franck−Condon transition energy of the mth pigment is obtained as

$$E_m^{\mathrm{abs}} = \langle \hat{H}_{me} - \hat{H}_{mg}\rangle_{mg} \tag{1}$$

where the canonical average has been introduced, $\langle\cdots\rangle = \mathrm{Tr}(\cdots\rho_{ma}^{\mathrm{eq}})$ with the environmental equilibrium state for the $|\varphi_{ma}\rangle$ state, $\hat{\rho}_{ma}^{\mathrm{eq}} = \mathrm{e}^{-\beta\hat{H}_{ma}}/(\mathrm{Tr}\ \mathrm{e}^{-\beta\hat{H}_{ma}})$. Here, β is the inverse temperature, $1/k_{\mathrm{B}}T$. The electronic energy of each diabatic state experiences fluctuations caused by the environmental and nuclear dynamics; these dynamics are described by the collective energy gap coordinate, such that

$$\hat{X}_m = \hat{H}_{me} - \hat{H}_{mg} - E_m^{\mathrm{abs}} \tag{2}$$

This coordinate is also employed for deriving quantum dynamic equations to simulate EET influenced by the environmental and nuclear dynamics,[64] and the relation with the spectral density is presented in the Appendix. By definition, the mean values of the coordinate with respect to the electronic ground and excited states are given by

$$\mu_{mg} = \langle \hat{X}_m\rangle_{mg} = 0 \tag{3a}$$

$$\mu_{me} = \langle \hat{X}_m\rangle_{me} = E_m^{\mathrm{em}} - E_m^{\mathrm{abs}} \tag{3b}$$

respectively, where the emission energy has been introduced

$$E_m^{\mathrm{em}} = \langle \hat{H}_{me} - \hat{H}_{mg}\rangle_{me} \tag{4}$$

For the sake of simplicity, the contributions of intramolecular vibrational modes are not considered at the current stage. The vibrational contribution will be discussed later in the paper.

Statistics of Fluctuations in Electronic Energy. Let the probability distribution function for the classical collective energy gap coordinate X_m be $P_{ma}(X_m)$ when the system is in the $|\varphi_{ma}\rangle$ state. The corresponding free energy is given by $F_{ma}(X_m) = -k_{\mathrm{B}}T\ \ln\ P_{ma}(X_m) + \mathrm{const}$. In this work, it is assumed that the environmentally induced fluctuations can be described as Gaussian random variables.[88,89] Under the assumption, the probability distribution function $P_{ma}(X_m)$ is expressed as

$$P_{ma}(X_m) \propto \exp\left[-\frac{1}{2\sigma_{ma}^2}(X_m - \mu_{ma})^2\right] \tag{5}$$

where σ_{ma}^2 denotes the variance of X_m with respect to the equilibrium state associated with the $|\varphi_{ma}\rangle$ state. Hence, the free energy with respect to X_m is given as a quadratic function

https://doi.org/10.1021/acs.jpcb.0c09847
J. Phys. Chem. B 2021, 125, 3286−3295

$$F_{ma}(X_m) = \frac{k_B T}{2\sigma_{ma}^2}(X_m - \mu_{ma})^2 + \text{const} \tag{6}$$

and the environmental reorganization energy associated with the optical transition to the $|\varphi_{ma}\rangle$ state, $E_{ma}^R = |F_{ma}(\mu_{mg}) - F_{ma}(\mu_{me})|$, is obtained as

$$E_{ma}^R = \frac{k_B T}{2\sigma_{ma}^2}(\mu_{me} - \mu_{mg})^2 \tag{7}$$

As described in the Appendix, the relation $\mu_{me} = -\beta\sigma_{mg}^2$ is valid under the Gaussian assumption, and the variances and hence the reorganization energies are independent of the electronic states, namely, $\sigma_{mg}^2 = \sigma_{me}^2 = \sigma_m^2$ and $E_{mg}^R = E_{me}^R = E_m^R$. Hence, eqs 3 and 7 lead to

$$E_m^{abs} - E_m^{em} = 2E_m^R \tag{8}$$

and a simple relation among the variance of the fluctuations σ_m^2, temperature T, and the reorganization energy E^R is obtained:

$$\sigma_m^2 = k_B T 2E_m^R \tag{9}$$

Consequently, the expressions of the free energies for the electronic ground and excited states are obtained as[88]

$$F_{mg}(X_m) = \frac{1}{4E_m^R}X_m^2 \tag{10a}$$

$$F_{me}(X_m) = E_m^{abs} - E_m^R + \frac{1}{4E_m^R}(X_m + 2E_m^R)^2 \tag{10b}$$

These expressions are consistent with the environmental dynamics in which the electronic and environmental states relax from the equilibrium configuration with respect to the $|\varphi_{mg}\rangle$ state and to the actual equilibrium configuration in the $|\varphi_{me}\rangle$ state after the vertical Franck–Condon excitation, as is formulated in the Appendix.

FREE ENERGY FOR PHOTOSYNTHETIC ENERGY TRANSFER

Free Energy of Activation Required for EET to Proceed. There is no experimental evidence of nonadiabatic transitions and radiative/nonradiative decays between $|\varphi_{me}\rangle$ and $|\varphi_{mg}\rangle$ in light harvesting pigment–protein complexes on the picosecond time scales, and hence, we organize the product states in order of elementary excitation number. The overall ground state with zero excitation is $|0\rangle = \prod_{m=1}^N |\varphi_{mg}\rangle$, whereas the presence of a single excitation at the mth pigment is expressed as $|m\rangle = |\varphi_{me}\rangle \prod_{k(\neq m)}|\varphi_{kg}\rangle$. The corresponding expansion of the complete PPC Hamiltonian yields $\hat{H}_{PPC} = \hat{H}_{PPC}^{(0)} + \hat{H}_{PPC}^{(1)} + \cdots$, where $\hat{H}_{PPC}^{(n)}$ describes n-excitation manifold comprising n elementary excitations. The Hamiltonian of the zero-excitation manifold is

$$\hat{H}_{PPC}^{(0)} = \hat{H}^{(0)}|0\rangle\langle 0| \tag{11}$$

with $\hat{H}^{(0)} = \sum_{m=1}^N \hat{H}_{mg}$. The Hamiltonian of the one-excitation manifold takes the form

$$\hat{H}_{PPC}^{(1)} = \sum_{m=1}^N \hat{H}_m|m\rangle\langle m| + \sum_{m,n} J_{mn}|m\rangle\langle n| \tag{12}$$

where $\hat{H}_m$ has been introduced as

$$\hat{H}_m = \hat{H}_{me} + \sum_{k(\neq m)} \hat{H}_{kg} = E_m^{abs} + \hat{X}_m + \hat{H}^{(0)} \tag{13}$$

The intensity of sunlight is weak, and thus, the single-excitation manifold is of primary importance under physiological conditions, although nonlinear spectroscopic techniques such as 2D electronic spectroscopy can populate higher excitation manifolds.

Correspondingly to the Hamiltonians, the free-energy surfaces for the zero- and one-excitation manifolds are given as

$$F^{(0)}(\mathbf{X}) = \sum_{m=1}^N F_{mg}(X_m) \tag{14}$$

$$F^{(1)}(\mathbf{X}) = \sum_{m=1}^N F_m(\mathbf{X})|m\rangle\langle m| + \sum_{m,n} J_{mn}|m\rangle\langle n| \tag{15}$$

where the free energy $F_m(\mathbf{X})$ has been introduced correspondingly to the Hamiltonian in eq 13 as

$$F_m(\mathbf{X}) = F_{me}(X_m) + \sum_{k(\neq m)} F_{kg}(X_k) = E_m^{abs} + X_m + F^{(0)}(\mathbf{X}) \tag{16}$$

For simplicity, the study addresses a dimer comprising pigments 1 and 2 and considers the two-dimensional reaction coordinate space, $\mathbf{X} = (X_1, X_2)$. In this case, eq 15 is easily diagonalized, and the adiabatic free-energy surfaces in the one-excitation manifold are obtained as

$$F_{\pm}(X_1, X_2) = \frac{F_1(\mathbf{X}) + F_2(\mathbf{X})}{2} \pm \sqrt{\left[\frac{F_1(\mathbf{X}) - F_2(\mathbf{X})}{2}\right]^2 + J_{12}^2} \tag{17}$$

The lower adiabatic free-energy surface $F_-(X_1, X_2)$ may possess two local minima corresponding to the environmental equilibria associated with states $|1\rangle = |\varphi_{1e}\rangle|\varphi_{2g}\rangle$ and $|2\rangle = |\varphi_{1g}\rangle|\varphi_{2e}\rangle$. Figure 1 draws an example of the adiabatic free-energy surface as a function of the two collective energy gap coordinates, X_1 and X_2. To highlight the two local minima, the parameters are chosen to be $E_1^{abs} - E_2^{abs} = 100\ \text{cm}^{-1}$, $J_{12} = -10\ \text{cm}^{-1}$, and $E_1^R = E_2^R = 500\ \text{cm}^{-1}$, although the values employed for the reorganization energies are large compared with typical ones for photosynthetic pigment–protein complexes, as will be discussed in Figure 2. The point of origin corresponds to the Franck–Condon state. The free energy of the point is higher than the barrier between the minima; therefore, delocalized excitons may be found immediately after the excitation even in the Förster regime.[90] As time increases, dissipation of reorganization energy proceeds, and the excitation will fall into one of the minima and become localized. This process can be described with the nonequilibrium energy difference given in eqs A9–A11. Subsequently, incoherent hopping EET takes place from one minimum to another and requires overcoming the free-energy barrier via thermal activation. Furthermore, eqs 10, 15, and 17 indicate that a decrease in the reorganization energy and an increase in the electronic coupling can reduce the barrier, leading to the maintenance of the delocalized excitons.

A question naturally arises concerning the height of the free-energy barrier or the free energy of activation. In the absence of the electronic coupling, the intersection of the diabatic free-energy surfaces, $F_1(X_1, X_2)$ and $F_2(X_1, X_2)$, is expressed as $X_1 + E_1^R = X_2 + E_2^R$, and the coordinates of the saddle point are given

https://doi.org/10.1021/acs.jpcb.0c09847
J. Phys. Chem. B 2021, 125, 3286–3295

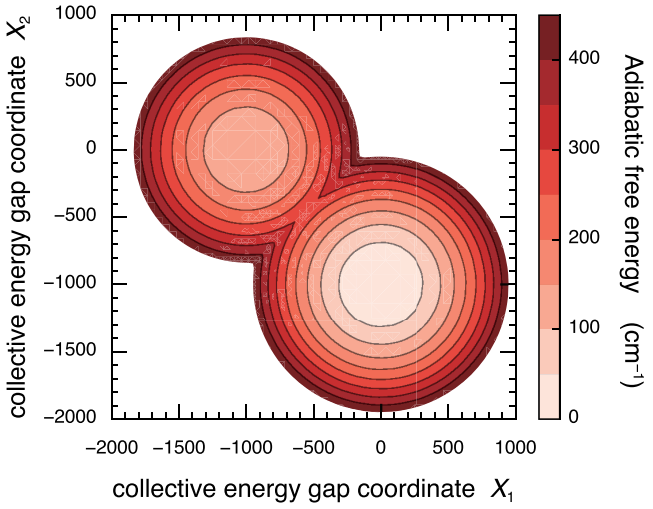

Figure 1. Example of the adiabatic free-energy surface of a dimer as a function of the two collective energy gap coordinates, X_1 and X_2, which describe fluctuations in the electronic energies. The parameters are chosen to be $E_1^{abs} - E_2^{abs} = 100$ cm^{-1}, $J_{12} = -10$ cm^{-1}, and $E_1^R - E_2^R = 500$ cm^{-1}. Contour lines are drawn at 50 cm^{-1} intervals. The adiabatic free-energy surface $F_-(X_1, X_2)$ typically possesses two local minima corresponding to the environmental equilibria associated with states $|1\rangle = |\varphi_{1e}\rangle|\varphi_{2g}\rangle$ and $|2\rangle = |\varphi_{1g}\rangle|\varphi_{2e}\rangle$. The point of origin corresponds to the Franck−Condon state. Incoherent hopping EET takes place from one minimum to another and requires overcoming the free-energy barrier via thermal activation.

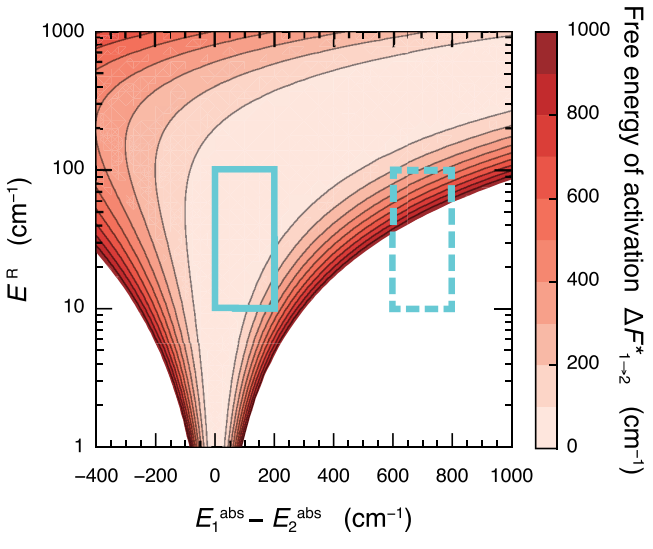

Figure 2. Contour plot of the free energy of activation required for the electronic energy transfer to proceed. The free energy of activation $\Delta F^*_{1\to2}$ is plotted as a function of the difference between the absorption energies $E_1^{abs} - E_2^{abs}$ and the reorganization energy $E^R = E_1^R = E_2^R$. Contour lines are drawn at 100 cm^{-1} intervals. The box with the solid line indicates the typical values for the photosynthetic electronic energy transfer, $0 \le E_1^{abs} - E_2^{abs} \le 200$ and 10 cm^{-1} $\le E^R \le$ 100 cm^{-1}. The thermal energy is evaluated as $k_BT \simeq 200$ cm^{-1} at physiological temperature $T = 300$ K, and therefore, for energy gap $\lesssim$ 200 cm^{-1} EET takes place in an almost activationless fashion in the parameter region corresponding to natural photosynthesis. For a large energy gap, an activation free energy is required (dashed box).

by $X_1^* = E_1^R(E_2^{abs} - E_1^{abs} - 2E_2^R)/(E_1^R + E_2^R)$, and $X_2^* = E_2^R(E_1^{abs} - E_2^{abs} - 2E_1^R)/(E_1^R + E_2^R)$. Hence, the height of the free-energy barrier associated with the transfer from pigments 1 to 2 is given by a simple formula similar to the Marcus' energy gap law

$$\Delta F^*_{1\to2} = \frac{(E_1^{abs} - E_2^{abs} - 2E_1^R)^2}{4(E_1^R + E_2^R)} \tag{18}$$

In deriving eq 18, the electronic coupling J_{mn} has been assumed to be vanishingly small for simplicity; however, eq 17 indicates that a finite value of the coupling lowers the free-energy barrier by approximately $|J_{12}|$. Therefore, eq 18 gives the supremum of the free energy of activation. Equation 18 is regarded as a multidimensional extension of Marcus theory; however, it can be recast in terms of the donor emission energy as $\Delta F^*_{1\to2} = (E_1^{em} - E_2^{abs})^2/4(E_1^R + E_2^R)$. This is physically consistent with the Förster rate formula expressed by the overlap integral of the donor-emission line shape $F_1(\omega)$ and the acceptor-absorption line shape $A_2(\omega)$. In this fashion, the free-energy profile can provide us with insights into the environment-induced fluctuations governing the EET processes. However, it is also noted that the adiabatic free-energy description could lead to a wrong insight when the reorganization time constant τ_{env} is sufficiently short in comparison to the inverse of the intersite electronic coupling, J_{12}^{-1}, as was investigated in ref 91.

Figure 2 presents the free energy of activation, $\Delta F^*_{1\to2}$, as a function of the reorganization energy, $E^R = E_1^R = E_2^R$, and the absorption energy difference, $E_1^{abs} - E_2^{abs}$. For typical values of $0 \le E_1^{abs} - E_2^{abs} \le 200$ and 10 cm^{-1} $\le E^R \le$ 100 cm^{-1},[92] the free energy of activation is very small in comparison to the thermal energy, $k_BT \simeq 200$ cm^{-1} at $T = 300$ K. In other words, EET takes place in a practically activationless fashion at physiological temperatures. This clarifies the physical origin of ultrafast EET. In Figure 2 of ref 69, it is shown that the EET rate in the case of $E_1^{abs} - E_2^{abs} = 100$ cm^{-1} is maximized for values of the reorganization energy typical in natural light harvesting systems. This optimization is consistent with the activationless nature of the free-energy surface. In natural light harvesting systems, there is a manifold of states. Although the coordinates involved span multiple dimensions, this can be visualized as relaxation down a slightly "bumpy" funnel in a rather similar fashion to the Wolynes' picture of protein folding landscapes.[93] Furthermore, the barrierless nature of the energy transfer over the wide range of parameters typical in natural light harvesting systems means that inhomogeneous broadening has rather little influence on the dynamics. The competence of protein environments to enable electronic excitation to flow in energetically and dynamically favorable manners was also addressed in a recent review by Jang and Mennucci.[94]

Coherent versus Incoherent. In the literature, the term "coherent transfer" indicates that excitation travels as a quantum mechanical wave packet keeping its phase coherence; otherwise, the term "incoherent transfer" is employed. As has been already discussed above, the incoherent "hopping" takes place from one minimum on the free-energy surface to another by overcoming a free-energy barrier that requires thermal activation. This is physically different from environment-induced destruction of the phase coherence. This point was also demonstrated with the use of a numerically accurate quantum dynamics calculation[69] and an approximate quantum-classical calculation[95] that was incapable of describing the free-energy barrier. As demonstrated in eq 18 and Figure 2, however, the barrier is insignificantly small in comparison to the thermal energy when energy gaps of $\lesssim$200 cm^{-1} are

https://doi.org/10.1021/acs.jpcb.0c09847
J. Phys. Chem. B 2021, 125, 3286−3295

considered, and thus, the EET takes place in a nearly activationless fashion. Although this transfer process does not have coherent dynamics in the sense of the macroscopic ensemble, the transfer is still mainly driven by the electronic interaction between the pigments rather than by the thermal activation although both of the electronic interaction and the environment-induced fluctuations play complementary roles. The absence of long-lasting oscillatory transients in the ensemble average does not necessarily provide a correct insight into the microscopic nature of the EET dynamics.[95] Therefore, activationless EET can be distinguished from genuine incoherent "hopping" that requires thermal activation.

The current approach also has an implication regarding the importance of the initial excitation, either by pulsed coherent light, by incoherent thermal light such as sunlight, or by energy transfer. If the barrier for energy transfer is substantial, the initial condition is influenced accordingly. That is, on a bumpy free-energy landscape with free-energy well traps, the initial state would determine the course of the EET. However, if the process is barrierless, the sensitivity on the initial condition is greatly reduced.

Vibrational Contribution. The examination of the free energy of activation can also provide an insight into the necessity of a vibrational contribution to assist the EET. In the case that the free energy of activation does not exceed the thermal energy, the EET can take place easily without the assistance of vibrational modes, even though spectroscopic measurements may detect vibrational and vibronic signatures. This situation corresponds to the parameter region marked with the solid line box in Figure 2. Indeed, ref 64 demonstrated that the electronic−vibrational quantum mixtures do not necessarily play a significant role in EET dynamics in the FMO complex, despite contributing to the enhancement of long-lived quantum beating in 2D electronic spectra. In other photosynthetic pigment−protein complexes, however, relatively large differences among the absorption energies are found, e.g., in light harvesting complex II (LHCII),[96−99] phycoerythrin 545,[15,38,100] and phycocyanin 645,[101−103] for which the vibrational contribution to assist the EET was investigated. Hence, we address the parameter region marked with the dashed line box in Figure 2, where 600 $cm^{-1} \leq E_1^{abs} - E_2^{abs} \leq 800$ and 10 $cm^{-1} \leq E^R \leq 100$ cm^{-1}. In this region, the free energy of activation is high compared to the thermal energy at physiological temperatures.

Some possible options for lowering the barrier with the fixed absorption energy difference are (1) an increase in the environmental reorganization energy E^R, (2) an increase in the intersite electronic coupling J_{mn}, (3) correlated fluctuations in electronic energies,[4,18] or (4) assistance by vibrational modes. When the energy acceptor is a vibrationally excited state of pigment 2, the absorption energy difference is reduced to $E_1^{abs} - (E_2^{abs} + \hbar\omega_{vib})$. In particular, the resonance between the vibrational frequency and the absorption energy difference leads to $E_1^{abs} - (E_2^{abs} + \hbar\omega_{vib}) = 0$, and thus, the free-energy barrier in Figure 2 is substantially lowered. When the Condon approximation is valid for the transition dipole moments, the interpigment coupling is reduced as $J_{mn} \rightarrow -J_{mn} e^{-S/2}\sqrt{S}$, with S being the Huang−Rhys factor of the vibrational mode. Nevertheless, a substantial rate enhancement by a high-frequency vibrational mode is possible, as demonstrated in Figure 3. This is consistent with the recent theoretical result on vibrationally assisted EET in LHCII.[98] When the non-Condon effect is more prominent, the effect results in the enhancement of the vibronic transitions,[104] possibly leading to the further acceleration of the vibrationally assisted EET.[99]

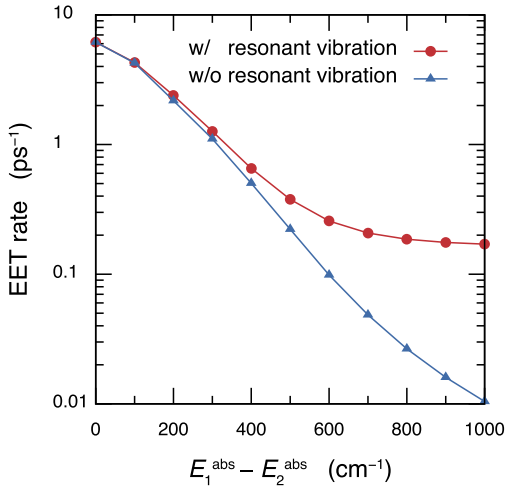

Figure 3. EET rate influenced by a resonant vibrational mode whose frequency is $\omega_{vib} = E_1^{abs} - E_2^{abs}$. The calculated rates are presented as a function of the absorption energy difference, $E_1^{abs} - E_2^{abs}$. They were obtained in the same fashion as in ref 64 with the following parameters: the intersite electronic coupling, J_{12} = 50 cm^{-1}; the environmental reorganization energy, the reorganization time constant, and the temperature set to λ_{env} = 35 cm^{-1}, τ_{env} = 100 fs, and T = 300 K, respectively; the vibrational relaxation time constant and the Huang−Rhys factor set to γ_{vib}^{-1} = 2 ps and S = 0.025, respectively. The Condon approximation was employed for the transition dipole moments.

Figure 3 presents the EET rate influenced by a resonant vibrational mode as a function of the absorption energy difference, $E_1^{abs} - E_2^{abs}$. These values were obtained in the same fashion as in ref 64 with the following parameters: the intersite electronic coupling, J_{12} = 50 cm^{-1}; the environmental reorganization energy, the reorganization time constant, and the temperature set to λ_{env} = 35 cm^{-1}, τ_{env} = 100 fs, and T = 300 K, respectively; and the vibrational relaxation time constant and the Huang−Rhys factor set to γ_{vib}^{-1} = 2 ps and S = 0.025, respectively. These parameters were taken from the model FMO complex,[64] and the Condon approximation was employed for the transition dipole moments. Consistent with the insight gained from the free-energy barrier in Figure 2, the extent of the vibrational assistance increases with increasing the value of $E_1^{abs} - E_2^{abs}$. Namely, the vibrational contribution strongly assists EET in the region of large absorption energy difference, even though it plays a minor role in the region of small absorption energy difference. Needless to say, vibrational modes with much larger Huang−Rhys factors and/or stronger electronic coupling would also play a bigger role even in the region of a small energy difference. However, the fuller study of such dependence lies outside the scope of this work. Here, it is noted that the vibrationally assisted EET rate exhibits a plateau in the region $E_1^{abs} - E_2^{abs} > 700$ cm^{-1}, indicating that the EET is promoted only by the vibrationally excited state. This can also be understood via the Förster rate formula. In the presence of a high-frequency vibrational mode, the absorption line shape of pigment 2 is expressed as $A_2(\omega) = A_2^{(0)}(\omega) + A_2^{(1)}(\omega) + \cdots$, where $A_2^{(v)}(\omega)$ is the line shape associated with the optical transition to the vth vibrational level in the electronically excited state and is approximately expressed as

https://doi.org/10.1021/acs.jpcb.0c09847
J. Phys. Chem. B 2021, 125, 3286−3295

$A_2^{(v)}(\omega) \simeq (S^v/v!)A_2^{(0)}(\omega - v\omega_{vib})$. In the case of high-frequency vibrational mode, the overlap between $A_2^{(0)}(\omega)$ and $A_2^{(1)}(\omega)$ vanishes, and hence, the vibrationally assisted EET rate is evaluated with the overlap integral between $F_1(\omega)$ and $A_2^{(1)}(\omega) = SA_2^{(0)}(\omega - \omega_{vib})$. It should be noted that the overlap integral is independent of the value of $E_1^{abs} - E_2^{abs}$ under the condition of $E_1^{abs} - E_2^{abs} = \omega_{vib}$.

CONCLUDING REMARKS

This paper presented a description of the photosynthetic energy transfer using a free-energy surface in order to understand the physical origins of its remarkable speed and to connect the complex quantum dynamical models to the intuitive picture of energy flow in photosynthetic pigment–protein complexes. Although it should be noted that real EET dynamics are not computed wth the free-energy surfaces, the free-energy profiles can still provide us with insights into the environment-induced fluctuations governing photosynthetic energy transfer processes. The presented free-energy description of ultrafast energy transfer reveals that photosynthetic systems operate in the barrierless regime when absorption energy differences among the pigments are $\lesssim$200 cm^{-1}. This makes the initial condition rather unimportant, suggesting that the method of excitation will not play a significant role in determining the microscopic processes. Our approach also provides insight into the necessity of the vibrational contribution and the distinction between coherent and incoherent energy transfer, showing that the absence of observable beats in the spectroscopy does not necessarily imply that the energy transfer is incoherent hopping. It is noted that the conclusions are valid when relatively weak electronic coupling, small Huang–Rhys factors, and the Condon approximation can be employed. Although these are often the appropriate regime for photosynthetic light harvesting, they are not always so. For such cases, more careful treatment should be necessary.

Although ways to electronically excite pigments will not play a significant role in determining the microscopic processes in the parameter region typical of photosynthetic light harvesting systems, it is still intriguing to elucidate how photoexcitation by natural light and the subsequent dynamics proceed with quantitative underpinnings. There are multiple spatiotemporal hierarchies related to the interaction between molecules and natural light, and thus, an issue similar to the above "coherent vs incoherent" issue is also present. In the time scales of direct human observation, sunlight photons continuously pump photosynthetic systems, and therefore, the excitation is sometimes considered as an incoherent continuous wave[105] or modeled as a photon bath.[106−108] As discussed in ref 109, however, the sunlight flux is estimated to be about 10 s^{-1} Å^{-2} at full sunlight, and the number of photons absorbed by a chlorophyll molecule is at most 10 s^{-1}. On subpicosecond and nanometer scales, consequently, the photon density is vanishingly small and a single photosynthetic pigment will be influenced by only a single photon.[110] In such a situation, photons may not be treated as continuous or pulsed waves in a classical manner, because the single-photon state $|\psi\rangle$ leads to $\langle\psi|\hat{E}(\mathbf{r}, t)|\psi\rangle = 0$ for the electric field operator, $\hat{E}(\mathbf{r}, t)$. Therefore, it might be necessary to take into account the quantum mechanical nature of the photons. Recently, a nonclassical Hong–Ou–Mandel interference between sunlight and single photons from a semiconductor quantum dot was experimentally demonstrated.[111] The theoretical investigation on pseudosunlight through the use of quantum entangled photons and its interaction with molecules[112] is also an attempt along this line. More elaborate investigations of photoexcitation by natural light and the subsequent excited-state dynamics in molecular systems are left for future studies.

APPENDIX

Static Properties of the Environmental Degrees of Freedom

The definition of the collective energy gap coordinate in eq 2 is recast into

$$\hat{H}_{me} = \hat{H}_{mg} + \hat{X}_m + E_{mg} \tag{A1}$$

Thus, $\hat{H}_{mg}$ and $\hat{X}_m$ may be regarded as an unperturbed system Hamiltonian and an external field, respectively. The linear response theory[113] allows an approximation of the environmental equilibrium state associated with $|\varphi_{me}\rangle$ as

$$\hat{\rho}_{me}^{eq} = \hat{\rho}_{mg}^{eq}\left(1 - \int_0^\beta d\lambda e^{\lambda\hat{H}_{mg}}\hat{X}_m e^{-\lambda\hat{H}_{mg}}\right) \tag{A2}$$

Consequently, the mean value of the collective energy gap coordinate with respect to the electronic excited state $\mu_{me} = \langle\hat{X}_m\rangle_{me}$ is evaluated as

$$\mu_{me} = -\beta\langle\hat{X}_m; \hat{X}_m\rangle_{mg} \tag{A3}$$

where $\langle\hat{X}_m\rangle_{mg} = 0$ in eq 3 has been employed, and $\langle\hat{O}_1; \hat{O}_2\rangle_{ma}$ stands for the canonical correlation[113] defined by $\langle\hat{O}_1; \hat{O}_2\rangle_{ma} = \beta^{-1}\int_0^\beta d\lambda\langle e^{\lambda\hat{H}_{ma}}\hat{O}_1 e^{-\lambda\hat{H}_{ma}}\hat{O}_2\rangle_{ma}$. In the classical limit of $\hbar \to 0$, the canonical correlation function can be approximated as the classical correlation function, and thus, eq A3 yields

$$\mu_{me} = -\beta\sigma_{mg}^2 \tag{A4}$$

Furthermore, the variance of the coordinate with respect to the electronic excited state is evaluated as

$$\sigma_{me}^2 = \langle\hat{X}_m^2\rangle_{me} = \mathrm{Tr}(\hat{X}_m^2\hat{\rho}_m^{eq}) = \langle\hat{X}_m^2\rangle_{mg} = \sigma_{mg}^2 \tag{A5}$$

where three-body correlation functions such as $\langle\hat{O}_m;\hat{O}_m^2\rangle_{mg}$ have vanished owing to the Gaussian statistics. As a consequence, eq 7 leads to $E_{mg}^R = E_{me}^R$.

Dynamic Properties of the Environmental Degrees of Freedom

After the electronic excitation in accordance with the vertical Franck–Condon transition, the electronic states and their surrounding environment reorganize from the equilibrium configuration with respect to the electronic ground state to reach the actual equilibrium configuration in the excited state. To formulate this process, let $\hat{\rho}_{me}(t)$ be the density operator that describes dynamics of the environmental DoFs associated with the electronically excited state of the mth pigment. The time-evolution after the photoexcitation at $t = 0$ is described with the Hamiltonian

$$\hat{H}_{me}(t) = \hat{H}_{mg} + (\hat{X}_m + E_{mg})\theta(t) \tag{A6}$$

with $\theta(t)$ being the Heaviside step function. Hence, the Liouville equation is written as

https://doi.org/10.1021/acs.jpcb.0c09847
J. Phys. Chem. B 2021, 125, 3286−3295

$$\frac{\partial}{\partial t}\hat{\rho}_{me}(t) = -\frac{i}{\hbar}[\hat{H}_{mg} + \hat{X}_m\theta(t), \hat{\rho}_{me}(t)] \tag{A7}$$

Similarly to the preceding section, $\hat{H}_{mg}$ and $\hat{X}_m\theta(t)$ can be regarded as an unperturbed system Hamiltonian and a time-dependent external field, respectively. The linear response theory[113] allows the approximation of $\hat{\rho}_{me}(t)$ as

$$\hat{\rho}_{me}(t) = \hat{\rho}_{mg}^{eq} - \frac{i}{\hbar}\int_0^t ds\hat{\mathcal{G}}_{mg}(t-s)[\hat{X}_m, \hat{\rho}_{mg}^{eq}] \tag{A8}$$

where $\hat{\mathcal{G}}_{mg}(t)$ is the time-evolution operator in the Liouville space, $\hat{\mathcal{G}}_{mg}(t)\hat{O} = e^{-i\hat{H}_{mg}t/\hbar}\hat{O}e^{i\hat{H}_{mg}t/\hbar}$, for any operator $\hat{O}$. The environmental dynamics can be measured by using the time-dependent fluorescence Stokes shift experiment. The experiment records the nonequilibrium energy difference between the electronic ground and excited states as a function of the delay time t after the photoexcitation,

$$\Delta E_m(t) = \mathrm{Tr}[(\hat{H}_{me} - \hat{H}_{mg})\hat{\rho}_{me}(t)] \tag{A9}$$

Substituting eq A8, we obtain

$$\Delta E_m(t) = E_m^{abs} - \Psi_m(0) + \Psi_m(t) \tag{A10}$$

with $\Psi_m(t)$ being the relaxation function defined by

$$\Psi_m(t) = \beta\langle\tilde{X}_m(t); \tilde{X}_m(0)\rangle_{mg} \tag{A11}$$

where the notation $\tilde{X}_m(t) = e^{i\hat{H}_{mg}t/\hbar}\tilde{X}_m(t)e^{i\hat{H}_{mg}t/\hbar}$ has been introduced. According to eqs A3 and 3a, the identity $\Psi_m(0) = -\mu_{me} = E_m^{abs} - E_m^{em}$ holds valid. Typically, the relaxation function $\Psi_m(t)$ converges to 0 in the long time limit, and therefore, $\Delta E(0) = E_m^{abs}$ and $\Delta E(\infty) = E_m^{em}$ are obtained. The spectral density is defined as the imaginary component of the susceptibility,[113] and hence, it is expressed in terms of the relaxation function, eq A11, as[64]

$$J_m(\omega) = \omega\int_0^\infty d\omega\Psi_m(t)\cos\omega t \tag{A12}$$

It should be noted that the relaxation function and spectral density contain the same information on the environment-induced fluctuations and vibrational modes affecting the electronic energy. The functions are independent of temperature. The relaxation function is inversely written as $\Psi_m(t) = (2/\pi)\int_0^\infty d\omega J_m(\omega)\omega^{-1}\cos\omega t$, leading to the widely employed relation between the reorganization energy and spectral density

$$E_m^R = \int_0^\infty d\omega\frac{J_m(\omega)}{\pi\omega} \tag{A13}$$

AUTHOR INFORMATION

Corresponding Authors

Akihito Ishizaki − *Institute for Molecular Science, National Institutes of Natural Sciences, Okazaki 444-8585, Japan; School of Physical Sciences, Graduate University for Advanced Studies, Okazaki 444-8585, Japan;* orcid.org/0000-0002-0246-4461; Email: ishizaki@ims.ac.jp

Graham R. Fleming − *Department of Chemistry, University of California, Berkeley, California 94720, United States; Molecular Biophysics and Integrated Bioimaging Division, Lawrence Berkeley National Laboratory, Berkeley, California 94720, United States; Kavli Energy NanoSciences Institute at Berkeley, Berkeley, California 94720, United States;* orcid.org/0000-0003-0847-1838; Email: grfleming@lbl.gov

Complete contact information is available at: https://pubs.acs.org/10.1021/acs.jpcb.0c09847

Notes

The authors declare no competing financial interest.

ACKNOWLEDGMENTS

The authors are grateful to Yuta Fujihashi for assistance with the figures. This work was supported by JSPS KAKENHI Grant 17H02946, MEXT KAKENHI Grant 17H06437 in Innovative Areas "Innovations for Light-Energy Conversion", and MEXT Quantum Leap Flagship Program Grant JPMXS0120330644. G.R.F.'s contribution was supported by the US Department of Energy, Office of Science, Basic Energy Sciences, Division of Chemical Sciences, Geosciences, and Biosciences.

REFERENCES

(1) Brixner, T.; Stenger, J.; Vaswani, H. M.; Cho, M.; Blankenship, R. E.; Fleming, G. R. Two-dimensional spectroscopy of electronic couplings in photosynthesis. *Nature* **2005**, *434*, 625−628.

(2) Cho, M.; Vaswani, H. M.; Brixner, T.; Stenger, J.; Fleming, G. R. Exciton Analysis in 2D Electronic Spectroscopy. *J. Phys. Chem. B* **2005**, *109*, 10542−10556.

(3) Engel, G. S.; Calhoun, T. R.; Read, E. L.; Ahn, T. K.; Mančal, T.; Cheng, Y.-C.; Blankenship, R. E.; Fleming, G. R. Evidence for wavelike energy transfer through quantum coherence in photosynthetic systems. *Nature* **2007**, *446*, 782−786.

(4) Lee, H.; Cheng, Y.-C.; Fleming, G. R. Coherence dynamics in photosynthesis: Protein protection of excitonic coherence. *Science* **2007**, *316*, 1462−1465.

(5) Calhoun, T. R.; Ginsberg, N. S.; Schlau-Cohen, G. S.; Cheng, Y.-C.; Ballottari, M.; Bassi, R.; Fleming, G. R. Quantum coherence enabled determination of the energy landscape in Light-Harvesting Complex II. *J. Phys. Chem. B* **2009**, *113*, 16291−16295.

(6) Savikhin, S.; Buck, D. R.; Struve, W. S. Oscillating anisotropies in a bacteriochlorophyll protein: Evidence for quantum beating between exciton levels. *Chem. Phys.* **1997**, *223*, 303−312.

(7) Olaya-Castro, A.; Lee, C.; Olsen, F.; Johnson, N. Efficiency of energy transfer in a light-harvesting system under quantum coherence. *Phys. Rev. B: Condens. Matter Mater. Phys.* **2008**, *78*, 085115.

(8) Mohseni, M.; Rebentrost, P.; Lloyd, S.; Aspuru-Guzik, A. Environment-assisted quantum walks in photosynthetic energy transfer. *J. Chem. Phys.* **2008**, *129*, 174106.

(9) Plenio, M. B.; Huelga, S. F. Dephasing-assisted transport: quantum networks and biomolecules. *New J. Phys.* **2008**, *10*, 113019.

(10) Rebentrost, P.; Mohseni, M.; Kassal, I.; Lloyd, S.; Aspuru-Guzik, A. Environment-assisted quantum transport. *New J. Phys.* **2009**, *11*, 033003.

(11) Ishizaki, A.; Fleming, G. R. Theoretical examination of quantum coherence in a photosynthetic system at physiological temperature. *Proc. Natl. Acad. Sci. U. S. A.* **2009**, *106*, 17255−17260.

(12) Nazir, A. Correlation-Dependent Coherent to Incoherent Transitions in Resonant Energy Transfer Dynamics. *Phys. Rev. Lett.* **2009**, *103*, 146404−4.

(13) Caruso, F.; Chin, A. W.; Datta, A.; Huelga, S. F.; Plenio, M. B. Highly efficient energy excitation transfer in light-harvesting complexes: The fundamental role of noise-assisted transport. *J. Chem. Phys.* **2009**, *131*, 105106.

(14) Panitchayangkoon, G.; Hayes, D.; Fransted, K. A.; Caram, J. R.; Harel, E.; Wen, J.; Blankenship, R. E.; Engel, G. S. Long-lived quantum coherence in photosynthetic complexes at physiological temperature. *Proc. Natl. Acad. Sci. U. S. A.* **2010**, *107*, 12766−12770.

(15) Collini, E.; Wong, C. Y.; Wilk, K. E.; Curmi, P. M. G.; Brumer, P.; Scholes, G. D. Coherently wired light-harvesting in photosynthetic marine algae at ambient temperature. *Nature* **2010**, *463*, 644−647.
(16) Caruso, F.; Chin, A. W.; Datta, A.; Huelga, S. F.; Plenio, M. B. Entanglement and entangling power of the dynamics in light-harvesting complexes. *Phys. Rev. A: At., Mol., Opt. Phys.* **2010**, *81*, 062346.
(17) Sarovar, M.; Ishizaki, A.; Fleming, G. R.; Whaley, K. B. Quantum entanglement in photosynthetic light-harvesting complexes. *Nat. Phys.* **2010**, *6*, 462−467.
(18) Ishizaki, A.; Fleming, G. R. Quantum superpositions in photosynthetic light harvesting: Delocalization and entanglement. *New J. Phys.* **2010**, *12*, 055004.
(19) Hoyer, S.; Sarovar, M.; Birgitta Whaley, K. Limits of quantum speedup in photosynthetic light harvesting. *New J. Phys.* **2010**, *12*, 065041.
(20) Fassioli, F.; Nazir, A.; Olaya-Castro, A. Quantum State Tuning of Energy Transfer in a Correlated Environment. *J. Phys. Chem. Lett.* **2010**, *1*, 2139−2143.
(21) Abramavicius, D.; Mukamel, S. Quantum oscillatory exciton migration in photosynthetic reaction centers. *J. Chem. Phys.* **2010**, *133*, 064510.
(22) Whaley, K. B.; Sarovar, M.; Ishizaki, A. Quantum entanglement phenomena in photosynthetic light harvesting complexes. *Procedia Chem.* **2011**, *3*, 152−164.
(23) Panitchayangkoon, G.; Voronine, D. V.; Abramavicius, D.; Caram, J. R.; Lewis, N. H. C.; Mukamel, S.; Engel, G. S. Direct evidence of quantum transport in photosynthetic light-harvesting complexes. *Proc. Natl. Acad. Sci. U. S. A.* **2011**, *108*, 20908−20912.
(24) Scholak, T.; de Melo, F.; Wellens, T.; Mintert, F.; Buchleitner, A. Efficient and coherent excitation transfer across disordered molecular networks. *Phys. Rev. E* **2011**, *83*, 021912.
(25) Schlau-Cohen, G. S.; Ishizaki, A.; Calhoun, T. R.; Ginsberg, N. S.; Ballottari, M.; Bassi, R.; Fleming, G. R. Elucidation of the timescales and origins of quantum electronic coherence in LHCII. *Nat. Chem.* **2012**, *4*, 389−395.
(26) Lewis, K. L. M.; Ogilvie, J. P. Probing Photosynthetic Energy and Charge Transfer with Two-Dimensional Electronic Spectroscopy. *J. Phys. Chem. Lett.* **2012**, *3*, 503−510.
(27) Westenhoff, S.; Paleček, D.; Edlund, P.; Smith, P.; Zigmantas, D. Coherent Picosecond Exciton Dynamics in a Photosynthetic Reaction Center. *J. Am. Chem. Soc.* **2012**, *134*, 16484−16487.
(28) Dawlaty, J. M.; Ishizaki, A.; De, A. K.; Fleming, G. R. Microscopic quantum coherence in a photosynthetic-light-harvesting antenna. *Philos. Trans. R. Soc., A* **2012**, *370*, 3672−3691.
(29) Chang, H.-T.; Cheng, Y.-C. Coherent versus incoherent excitation energy transfer in molecular systems. *J. Chem. Phys.* **2012**, *137*, 165103.
(30) Hoyer, S.; Ishizaki, A.; Whaley, K. B. Spatial propagation of excitonic coherence enables ratcheted energy transfer. *Phys. Rev. E* **2012**, *86*, 041911.
(31) Shabani, A.; Mohseni, M.; Rabitz, H.; Lloyd, S. Efficient estimation of energy transfer efficiency in light-harvesting complexes. *Phys. Rev. E* **2012**, *86*, 011915.
(32) Wu, J.; Liu, F.; Ma, J.; Silbey, R. J.; Cao, J. Efficient energy transfer in light-harvesting systems: Quantum-classical comparison, flux network, and robustness analysis. *J. Chem. Phys.* **2012**, *137*, 174111.
(33) Dijkstra, A. G.; Tanimura, Y. The role of the environment time scale in light-harvesting efficiency and coherent oscillations. *New J. Phys.* **2012**, *14*, 073027−12.
(34) Hildner, R.; Brinks, D.; Nieder, J. B.; Cogdell, R. J.; van Hulst, N. F. Quantum Coherent Energy Transfer over Varying Pathways in Single Light-Harvesting Complexes. *Science* **2013**, *340*, 1448−1451.
(35) Chin, A. W.; Prior, J.; Rosenbach, R.; Caycedo-Soler, F.; Huelga, S. F.; Plenio, M. B. The role of non-equilibrium vibrational structures in electronic coherence and recoherence in pigment-protein complexes. *Nat. Phys.* **2013**, *9*, 113−118.
(36) Gelzinis, A.; Valkunas, L.; Fuller, F. D.; Ogilvie, J. P.; Mukamel, S.; Abramavicius, D. Tight-binding model of the photosystem II reaction center: Application to two-dimensional electronic spectroscopy. *New J. Phys.* **2013**, *15*, 075013.
(37) Rivera, E.; Montemayor, D.; Masia, M.; Coker, D. F. Influence of Site-Dependent Pigment-Protein Interactions on Excitation Energy Transfer in Photosynthetic Light Harvesting. *J. Phys. Chem. B* **2013**, *117*, 5510−5521.
(38) O'Reilly, E. J.; Olaya-Castro, A. Non-classicality of the molecular vibrations assisting exciton energy transfer at room temperature. *Nat. Commun.* **2014**, *5*, 3012.
(39) De, A. K.; Monahan, D.; Dawlaty, J. M.; Fleming, G. R. Two-dimensional fluorescence-detected coherent spectroscopy with absolute phasing by confocal imaging of a dynamic grating and 27-step phase-cycling. *J. Chem. Phys.* **2014**, *140*, 194201−9.
(40) Dijkstra, A. G.; Tanimura, Y. Linear and third- and fifth-order nonlinear spectroscopies of a charge transfer system coupled to an underdamped vibration. *J. Chem. Phys.* **2015**, *142*, 212423−8.
(41) Scholes, G. D.; et al. Using coherence to enhance function in chemical and biophysical systems. *Nature* **2017**, *543*, 647−656.
(42) Knee, G. C.; Rowe, P.; Smith, L. D.; Troisi, A.; Datta, A. Structure-Dynamics Relation in Physically-Plausible Multi-Chromophore Systems. *J. Phys. Chem. Lett.* **2017**, *8*, 2328−2333.
(43) Dutta, R.; Bagchi, B. Environment-Assisted Quantum Coherence in Photosynthetic Complex. *J. Phys. Chem. Lett.* **2017**, *8*, 5566−5572.
(44) Sakamoto, S.; Tanimura, Y. Exciton-Coupled Electron Transfer Process Controlled by Non-Markovian Environments. *J. Phys. Chem. Lett.* **2017**, *8*, 5390−5394.
(45) Thyrhaug, E.; Tempelaar, R.; Alcocer, M. J. P.; Žídek, K.; Bína, D.; Knoester, J.; Jansen, T. L. C.; Zigmantas, D. Identification and characterization of diverse coherences in the Fenna-Matthews-Olson complex. *Nat. Chem.* **2018**, *10*, 780−786.
(46) Saito, S.; Higashi, M.; Fleming, G. R. Site-Dependent Fluctuations Optimize Electronic Energy Transfer in the Fenna-Matthews-Olson Protein. *J. Phys. Chem. B* **2019**, *123*, 9762−9772.
(47) Kim, C. W.; Lee, W.-G.; Kim, I.; Rhee, Y. M. Effect of Underdamped Vibration on Excitation Energy Transfer: Direct Comparison between Two Different Partitioning Schemes. *J. Phys. Chem. A* **2019**, *123*, 1186−1197.
(48) Sanchez Muñoz, C. S.; Schlawin, F. Photon Correlation Spectroscopy as a Witness for Quantum Coherence. *Phys. Rev. Lett.* **2020**, *124*, 203601.
(49) Cao, J.; et al. Quantum biology revisited. *Science Advances* **2020**, *6*, No. eaaz4888.
(50) Chan, W.-L.; Berkelbach, T. C.; Provorse, M. R.; Monahan, N. R.; Tritsch, J. R.; Hybertsen, M. S.; Reichman, D. R.; Gao, J.; Zhu, X. Y. The quantum coherent mechanism for singlet fission: experiment and theory. *Acc. Chem. Res.* **2013**, *46*, 1321−1329.
(51) Gélinas, S.; Rao, A.; Kumar, A.; Smith, S. L.; Chin, A. W.; Clark, J.; van der Poll, T. S.; Bazan, G. C.; Friend, R. H. Ultrafast Long-Range Charge Separation in Organic Semiconductor Photovoltaic Diodes. *Science* **2014**, *343*, 512−516.
(52) Lee, M. H.; Aragó, J.; Troisi, A. Charge Dynamics in Organic Photovoltaic Materials: Interplay between Quantum Diffusion and Quantum Relaxation. *J. Phys. Chem. C* **2015**, *119*, 14989−14998.
(53) Bredas, J.-L.; Sargent, E. H.; Scholes, G. D. Photovoltaic concepts inspired by coherence effects in photosynthetic systems. *Nat. Mater.* **2017**, *16*, 35−44.
(54) Kato, A.; Ishizaki, A. Non-Markovian Quantum-Classical Ratchet for Ultrafast Long-Range Electron-Hole Separation in Condensed Phases. *Phys. Rev. Lett.* **2018**, *121*, 026001.
(55) Nemeth, A.; Milota, F.; Mančal, T.; Lukeš, V.; Hauer, J.; Kauffmann, H. F.; Sperling, J. Vibrational wave packet induced oscillations in two-dimensional electronic spectra. I. Experiments. *J. Chem. Phys.* **2010**, *132*, 184514.
(56) Mančal, T.; Nemeth, A.; Milota, F.; Lukeš, V.; Kauffmann, H. F.; Sperling, J. Vibrational wave packet induced oscillations in two-

https://doi.org/10.1021/acs.jpcb.0c09847
J. Phys. Chem. B 2021, 125, 3286−3295

dimensional electronic spectra. II. Theory. *J. Chem. Phys.* **2010**, *132*, 184515.
(57) Butkus, V.; Zigmantas, D.; Valkunas, L.; Abramavicius, D. Vibrational vs. electronic coherences in 2D spectrum of molecular systems. *Chem. Phys. Lett.* **2012**, *545*, 40−43.
(58) Yuen-Zhou, J.; Krich, J. J.; Aspuru-Guzik, A. A witness for coherent electronic vs vibronic-only oscillations in ultrafast spectroscopy. *J. Chem. Phys.* **2012**, *136*, 234501.
(59) Caycedo-Soler, F.; Chin, A. W.; Almeida, J.; Huelga, S. F.; Plenio, M. B. The nature of the low energy band of the Fenna-Matthews-Olson complex: Vibronic signatures. *J. Chem. Phys.* **2012**, *136*, 155102.
(60) Christensson, N.; Kauffmann, H. F.; Pullerits, T.; Mančal, T. Origin of Long-Lived Coherences in Light-Harvesting Complexes. *J. Phys. Chem. B* **2012**, *116*, 7449−7454.
(61) Tiwari, V.; Peters, W. K.; Jonas, D. M. Electronic resonance with anticorrelated pigment vibrations drives photosynthetic energy transfer outside the adiabatic framework. *Proc. Natl. Acad. Sci. U. S. A.* **2013**, *110*, 1203−1208.
(62) Romero, E.; Augulis, R.; Novoderezhkin, V. I.; Ferretti, M.; Thieme, J.; Zigmantas, D.; van Grondelle, R. Quantum coherence in photosynthesis for efficient solar-energy conversion. *Nat. Phys.* **2014**, *10*, 676−682.
(63) Fuller, F. D.; Pan, J.; Gelzinis, A.; Butkus, V.; Senlik, S. S.; Wilcox, D. E.; Yocum, C. F.; Valkunas, L.; Abramavicius, D.; Ogilvie, J. P. Vibronic coherence in oxygenic photosynthesis. *Nat. Chem.* **2014**, *6*, 706−711.
(64) Fujihashi, Y.; Fleming, G. R.; Ishizaki, A. Impact of environmentally induced fluctuations on quantum mechanically mixed electronic and vibrational pigment states in photosynthetic energy transfer and 2D electronic spectra. *J. Chem. Phys.* **2015**, *142*, 212403.
(65) Monahan, D. M.; Whaley-Mayda, L.; Ishizaki, A.; Fleming, G. R. Influence of weak vibrational-electronic couplings on 2D electronic spectra and inter-site coherence in weakly coupled photosynthetic complexes. *J. Chem. Phys.* **2015**, *143*, 065101.
(66) Fujihashi, Y.; Fleming, G. R.; Ishizaki, A. Influences of Quantum Mechanically Mixed Electronic and Vibrational Pigment States in 2D Electronic Spectra of Photosynthetic Systems: Strong Electronic Coupling Cases. *J. Chin. Chem. Soc.* **2016**, *63*, 49−56.
(67) Fujihashi, Y.; Higashi, M.; Ishizaki, A. Intramolecular Vibrations Complement the Robustness of Primary Charge Separation in a Dimer Model of the Photosystem II Reaction Center. *J. Phys. Chem. Lett.* **2018**, *9*, 4921−4929.
(68) Jang, S.; Cheng, Y.-C.; Reichman, D. R.; Eaves, J. D. Theory of coherent resonance energy transfer. *J. Chem. Phys.* **2008**, *129*, 101104.
(69) Ishizaki, A.; Fleming, G. R. Unified treatment of quantum coherent and incoherent hopping dynamics in electronic energy transfer: reduced hierarchy equation approach. *J. Chem. Phys.* **2009**, *130*, 234111.
(70) Prior, J.; Chin, A. W.; Huelga, S. F.; Plenio, M. B. Efficient Simulation of Strong System-Environment Interactions. *Phys. Rev. Lett.* **2010**, *105*, 050404.
(71) Huo, P.; Coker, D. F. Iterative linearized density matrix propagation for modeling coherent excitation energy transfer in photosynthetic light harvesting. *J. Chem. Phys.* **2010**, *133*, 184108.
(72) Tao, G.; Miller, W. H. Semiclassical Description of Electronic Excitation Population Transfer in a Model Photosynthetic System. *J. Phys. Chem. Lett.* **2010**, *1*, 891−894.
(73) Kelly, A.; Rhee, Y. M. Mixed Quantum-Classical Description of Excitation Energy Transfer in a Model Fenna-Matthews-Olsen Complex. *J. Phys. Chem. Lett.* **2011**, *2*, 808−812.
(74) Nalbach, P.; Ishizaki, A.; Fleming, G. R.; Thorwart, M. Iterative path-integral algorithm versus cumulant time-nonlocal master equation approach for dissipative biomolecular exciton transport. *New J. Phys.* **2011**, *13*, 063040.
(75) Berkelbach, T. C.; Markland, T. E.; Reichman, D. R. Reduced density matrix hybrid approach: Application to electronic energy transfer. *J. Chem. Phys.* **2012**, *136*, 084104.
(76) Kelly, A.; Markland, T. E. Efficient and accurate surface hopping for long time nonadiabatic quantum dynamics. *J. Chem. Phys.* **2013**, *139*, 014104.
(77) Banchi, L.; Costagliola, G.; Ishizaki, A.; Giorda, P. An analytical continuation approach for evaluating emission lineshapes of molecular aggregates and the adequacy of multichromophoric Förster theory. *J. Chem. Phys.* **2013**, *138*, 184107.
(78) Bhattacharyya, P.; Sebastian, K. L. Adiabatic eigenfunction-based approach for coherent excitation transfer: an almost analytical treatment of the Fenna-Matthews-Olson complex. *Phys. Rev. E* **2013**, *87*, 062712.
(79) Jang, S.; Hoyer, S.; Fleming, G. R.; Whaley, K. B. Generalized Master Equation with Non-Markovian Multichromophoric Förster Resonance Energy Transfer for Modular Exciton Densities. *Phys. Rev. Lett.* **2014**, *113*, 188102.
(80) Hwang-Fu, Y.-H.; Chen, W.; Cheng, Y.-C. A coherent modified Redfield theory for excitation energy transfer in molecular aggregates. *Chem. Phys.* **2015**, *447*, 46−53.
(81) Tamascelli, D.; Smirne, A.; Lim, J.; Huelga, S. F.; Plenio, M. B. Efficient Simulation of Finite-Temperature Open Quantum Systems. *Phys. Rev. Lett.* **2019**, *123*, 090402.
(82) Zhou, H. X.; Szabo, A. Microscopic formulation of Marcus' theory of electron transfer. *J. Chem. Phys.* **1995**, *103*, 3481−3494.
(83) Georgievskii, Y.; Hsu, C.-P.; Marcus, R. A. Linear response in theory of electron transfer reactions as an alternative to the molecular harmonic oscillator model. *J. Chem. Phys.* **1999**, *110*, 5307.
(84) Matyushov, D. V.; Voth, G. A. Modeling the free energy surfaces of electron transfer in condensed phases. *J. Chem. Phys.* **2000**, *113*, 5413−13.
(85) Jang, S.; Jung, Y. J.; Silbey, R. J. Nonequilibrium generalization of Förster-Dexter theory for excitation energy transfer. *Chem. Phys.* **2002**, *275*, 319.
(86) Matyushov, D. V. Protein electron transfer: Dynamics and statistics. *J. Chem. Phys.* **2013**, *139*, 025102−13.
(87) Adolphs, J.; Renger, T. How Proteins Trigger Excitation Energy Transfer in the FMO Complex of Green Sulfur Bacteria. *Biophys. J.* **2006**, *91*, 2778−2797.
(88) Marchi, M.; Gehlen, J. N.; Chandler, D.; Newton, M. Diabatic surfaces and the pathway for primary electron transfer in a photosynthetic reaction center. *J. Am. Chem. Soc.* **1993**, *115*, 4178−4190.
(89) Shim, S.; Rebentrost, P.; Valleau, S.; Aspuru-Guzik, A. Atomistic study of the long-lived quantum coherences in the Fenna-Matthews-Olson complex. *Biophys. J.* **2012**, *102*, 649−660.
(90) Ishizaki, A.; Calhoun, T. R.; Schlau-Cohen, G. S.; Fleming, G. R. Quantum coherence and its interplay with protein environments in photosynthetic electronic energy transfer. *Phys. Chem. Chem. Phys.* **2010**, *12*, 7319−7337.
(91) Ishizaki, A. Interactions between quantum mixing and the environmental dynamics controlling ultrafast photoinduced electron transfer and its temperature dependence. *Chem. Lett.* **2013**, *42*, 1406−1408.
(92) van Amerongen, H.; Valkunas, L.; van Grondelle, R. *Photosynthetic Excitons*; World Scientific: Singapore, 2000.
(93) Bryngelson, J. D.; Wolynes, P. G. Spin glasses and the statistical mechanics of protein folding. *Proc. Natl. Acad. Sci. U. S. A.* **1987**, *84*, 7524−7528.
(94) Jang, S. J.; Mennucci, B. Delocalized excitons in natural light-harvesting complexes. *Rev. Mod. Phys.* **2018**, *90*, 035003.
(95) Ishizaki, A.; Fleming, G. R. On the Interpretation of Quantum Coherent Beats Observed in Two-Dimensional Electronic Spectra of Photosynthetic Light Harvesting Complexes. *J. Phys. Chem. B* **2011**, *115*, 6227−6233.
(96) Novoderezhkin, V. I.; Palacios, M. A.; van Amerongen, H.; van Grondelle, R. Excitation Dynamics in the LHCII Complex of Higher Plants: Modeling Based on the 2.72 Å Crystal Structure. *J. Phys. Chem. B* **2005**, *109*, 10493−10504.
(97) Schlau-Cohen, G. S.; Calhoun, T. R.; Ginsberg, N. S.; Read, E. L.; Ballottari, M.; Bassi, R.; van Grondelle, R.; Fleming, G. R.

https://doi.org/10.1021/acs.jpcb.0c09847
J. Phys. Chem. B 2021, 125, 3286−3295

Pathways of Energy Flow in LHCII from Two-Dimensional Electronic Spectroscopy. *J. Phys. Chem. B* **2009**, *113*, 15352−15363.
(98) Bhattacharyya, P.; Fleming, G. R. The role of resonant nuclear modes in vibrationally assisted energy transport: The LHCII complex. *J. Chem. Phys.* **2020**, *153*, 044119.
(99) Arsenault, E. A.; Yoneda, Y.; Iwai, M.; Niyogi, K. K.; Fleming, G. R. Vibronic mixing enables ultrafast energy flow in light-harvesting complex II. *Nat. Commun.* **2020**, *11*, 1460.
(100) Kolli, A.; O'Reilly, E. J.; Scholes, G. D.; Olaya-Castro, A. The fundamental role of quantized vibrations in coherent light harvesting by cryptophyte algae. *J. Chem. Phys.* **2012**, *137*, 174109.
(101) Dean, J. C.; Mirkovic, T.; Toa, Z. S. D.; Oblinsky, D. G.; Scholes, G. D. Vibronic Enhancement of Algae Light Harvesting. *Chem.* **2016**, *1*, 858−872.
(102) Blau, S. M.; Bennett, D. I. G.; Kreisbeck, C.; Scholes, G. D.; Aspuru-Guzik, A. Local protein solvation drives direct down-conversion in phycobiliprotein PC645 via incoherent vibronic transport. *Proc. Natl. Acad. Sci. U. S. A.* **2018**, *115*, E3342−E3350.
(103) Bennett, D. I. G.; Malý, P.; Kreisbeck, C.; van Grondelle, R.; Aspuru-Guzik, A. Mechanistic Regimes of Vibronic Transport in a Heterodimer and the Design Principle of Incoherent Vibronic Transport in Phycobiliproteins. *J. Phys. Chem. Lett.* **2018**, *9*, 2665−2670.
(104) Zhang, H.-D.; Qiao, Q.; Xu, R.-X.; Yan, Y. Effects of Herzberg-Teller vibronic coupling on coherent excitation energy transfer. *J. Chem. Phys.* **2016**, *145*, 204109−9.
(105) Brumer, P.; Shapiro, M. Molecular response in one-photon absorption via natural thermal light vs. pulsed laser excitation. *Proc. Natl. Acad. Sci. U. S. A.* **2012**, *109*, 19575−19578.
(106) Mančal, T.; Valkunas, L. Exciton dynamics in photosynthetic complexes: excitation by coherent and incoherent light. *New J. Phys.* **2010**, *12*, 065044.
(107) Fassioli, F.; Olaya-Castro, A.; Scholes, G. D. Coherent Energy Transfer under Incoherent Light Conditions. *J. Phys. Chem. Lett.* **2012**, *3*, 3136−3142.
(108) Pachón, L. A.; Botero, J. D.; Brumer, P. Open system perspective on incoherent excitation of light-harvesting systems. *J. Phys. B: At., Mol. Opt. Phys.* **2017**, *50*, 184003.
(109) Blankenship, R. E. *Molecular Mechanisms of Photosynthesis*; Wiley Blackwell: West Sussex, U.K., 2013.
(110) Chan, H. C. H.; Gamel, O. E.; Fleming, G. R.; Whaley, K. B. Single-photon absorption by single photosynthetic light-harvesting complexes. *J. Phys. B: At., Mol. Opt. Phys.* **2018**, *51*, 054002.
(111) Deng, Y.-H.; et al. Quantum Interference between Light Sources Separated by 150 Million Kilometers. *Phys. Rev. Lett.* **2019**, *123*, 080401.
(112) Fujihashi, Y.; Shimizu, R.; Ishizaki, A. Generation of pseudo-sunlight via quantum entangled photons and the interaction with molecules. *Phys. Rev. Research* **2020**, *2*, 023256.
(113) Kubo, R.; Toda, M.; Hashitsume, N. *Statistical Physics II*; Springer: Berlin, 1985.

https://doi.org/10.1021/acs.jpcb.0c09847
J. Phys. Chem. B 2021, 125, 3286−3295